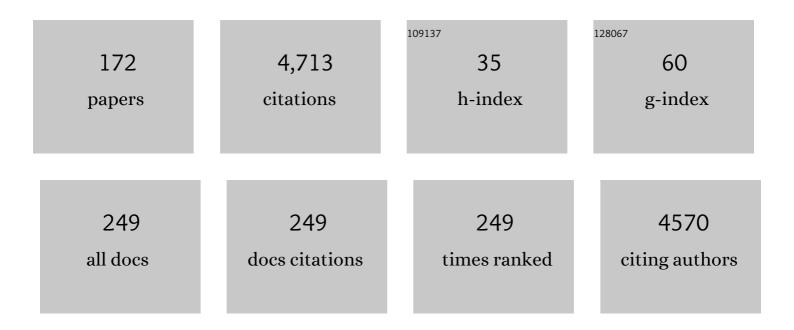
List of Publications by Year in descending order

Source: https://exaly.com/author-pdf/5508713/publications.pdf Version: 2024-02-01



PETER I H SCOTT

#	Article	IF	CITATIONS
1	Late-stage [¹⁸ F]fluorination: new solutions to old problems. Chemical Science, 2014, 5, 4545-4553.	3.7	266
2	Synthesis of [¹⁸ F]Arenes via the Copper-Mediated [¹⁸ F]Fluorination of Boronic Acids. Organic Letters, 2015, 17, 5780-5783.	2.4	199
3	Copper-Catalyzed [¹⁸ F]Fluorination of (Mesityl)(aryl)iodonium Salts. Organic Letters, 2014, 16, 3224-3227.	2.4	197
4	Gait speed in Parkinson disease correlates with cholinergic degeneration. Neurology, 2013, 81, 1611-1616.	1.5	185
5	Copper-Mediated Radiofluorination of Arylstannanes with [¹⁸ F]KF. Organic Letters, 2016, 18, 5440-5443.	2.4	151
6	Thalamic cholinergic innervation and postural sensory integration function in Parkinson's disease. Brain, 2013, 136, 3282-3289.	3.7	140
7	Frequency of Cholinergic and Caudate Nucleus Dopaminergic Deficits Across the Predemented Cognitive Spectrum of Parkinson Disease and Evidence of Interaction Effects. JAMA Neurology, 2015, 72, 194.	4.5	121
8	Radiosyntheses using Fluorine-18: The Art and Science of Late Stage Fluorination. Current Topics in Medicinal Chemistry, 2014, 14, 875-900.	1.0	121
9	In Vivo Imaging of Human Cholinergic Nerve Terminals with (–)-5- ¹⁸ F-Fluoroethoxybenzovesamicol: Biodistribution, Dosimetry, and Tracer Kinetic Analyses. Journal of Nuclear Medicine, 2014, 55, 396-404.	2.8	107
10	Extraâ€nigral pathological conditions are common in Parkinson's disease with freezing of gait: An <i>in vivo</i> positron emission tomography study. Movement Disorders, 2014, 29, 1118-1124.	2.2	101
11	Novel Strategies for Fluorineâ€18 Radiochemistry. Angewandte Chemie - International Edition, 2012, 51, 1106-1109.	7.2	96
12	Iridium atalysed Câ^'H Borylation of Heteroarenes: Balancing Steric and Electronic Regiocontrol. Angewandte Chemie - International Edition, 2021, 60, 2796-2821.	7.2	95
13	Cu-Mediated C–H ¹⁸ F-Fluorination of Electron-Rich (Hetero)arenes. Organic Letters, 2017, 19, 3939-3942.	2.4	87
14	High Affinity Radiopharmaceuticals Based Upon Lansoprazole for PET Imaging of Aggregated Tau in Alzheimer's Disease and Progressive Supranuclear Palsy: Synthesis, Preclinical Evaluation, and Lead Selection. ACS Chemical Neuroscience, 2014, 5, 718-730.	1.7	77
15	Highlighting the versatility of the tracerlab synthesis modules. Part 1: fully automated production of [¹⁸ F]labelled radiopharmaceuticals using a Tracerlab FX _{FN} . Journal of Labelled Compounds and Radiopharmaceuticals, 2011, 54, 292-307.	0.5	76
16	Methods for the Incorporation of Carbonâ€11 To Generate Radiopharmaceuticals for PET Imaging. Angewandte Chemie - International Edition, 2009, 48, 6001-6004.	7.2	72
17	Diabetes mellitus is independently associated with more severe cognitive impairment in Parkinson disease. Parkinsonism and Related Disorders, 2014, 20, 1394-1398.	1.1	71
18	Studies into radiolytic decomposition of fluorine-18 labeled radiopharmaceuticals for positron emission tomography. Applied Radiation and Isotopes, 2009, 67, 88-94.	0.7	58

#	Article	IF	CITATIONS
19	Clinical markers for identifying cholinergic deficits in Parkinson's disease. Movement Disorders, 2015, 30, 269-273.	2.2	54
20	Cyclotron-based production of 68Ga, [68Ga]GaCl3, and [68Ga]Ga-PSMA-11 from a liquid target. EJNMMI Radiopharmacy and Chemistry, 2020, 5, 25.	1.8	54
21	Highlighting the versatility of the Tracerlab synthesis modules. Part 2: fully automated production of [¹¹ C]″abeled radiopharmaceuticals using a Tracerlab FX _{Câ€Pro} . Journal of Labelled Compounds and Radiopharmaceuticals, 2011, 54, 819-838.	0.5	53
22	Evaluation of [¹¹ C] <i>N</i> -Methyl Lansoprazole as a Radiopharmaceutical for PET Imaging of Tau Neurofibrillary Tangles. ACS Medicinal Chemistry Letters, 2012, 3, 936-941.	1.3	52
23	Striatal and <scp>C</scp> ortical βâ€ <scp>A</scp> myloidopathy and <scp>C</scp> ognition in <scp>P</scp> arkinson's <scp>D</scp> isease. Movement Disorders, 2016, 31, 111-117.	2.2	52
24	Development of Customized [18F]Fluoride Elution Techniques for the Enhancement of Copper-Mediated Late-Stage Radiofluorination. Scientific Reports, 2017, 7, 233.	1.6	51
25	Clinical Applications of Radiolabeled Peptides for PET. Seminars in Nuclear Medicine, 2017, 47, 493-523.	2.5	49
26	Guidelines for the content and format of PET brain data in publications and archives: A consensus paper. Journal of Cerebral Blood Flow and Metabolism, 2020, 40, 1576-1585.	2.4	47
27	Moving Metal-Mediated ¹⁸ F-Fluorination from Concept to Clinic. ACS Central Science, 2016, 2, 128-130.	5.3	44
28	Copper-mediated late-stage radiofluorination: five years of impact on preclinical and clinical PET imaging. Clinical and Translational Imaging, 2020, 8, 167-206.	1.1	44
29	On the consensus nomenclature rules for radiopharmaceutical chemistry – Reconsideration of radiochemical conversion. Nuclear Medicine and Biology, 2021, 93, 19-21.	0.3	43
30	Diversity Linker Units for Solidâ€Phase Organic Synthesis. European Journal of Organic Chemistry, 2006, 2006, 2251-2268.	1.2	42
31	Classics in Neuroimaging: Development of PET Tracers for Imaging Monoamine Oxidases. ACS Chemical Neuroscience, 2019, 10, 1867-1871.	1.7	42
32	Copperâ€Mediated Aminoquinolineâ€Directed Radiofluorination of Aromatic Câ^'H Bonds with K ¹⁸ F. Angewandte Chemie - International Edition, 2019, 58, 3119-3122.	7.2	40
33	Fully automated preparation of [11C]choline and [18F]fluoromethylcholine using TracerLab synthesis modules and facilitated quality control using analytical HPLC. Applied Radiation and Isotopes, 2011, 69, 403-409.	0.7	38
34	Synthesis and Initial <i>in Vivo</i> Studies with [¹¹ C]SB-216763: The First Radiolabeled Brain Penetrative Inhibitor of GSK-3. ACS Medicinal Chemistry Letters, 2015, 6, 548-552.	1.3	38
35	Synthesis of Diverse ¹¹ C-Labeled PET Radiotracers via Direct Incorporation of [¹¹ C]CO ₂ . Bioconjugate Chemistry, 2016, 27, 1382-1389.	1.8	38
36	DARK Classics in Chemical Neuroscience: Cocaine. ACS Chemical Neuroscience, 2018, 9, 2358-2372.	1.7	38

#	Article	IF	CITATIONS
37	Identification of AV-1451 as a Weak, Nonselective Inhibitor of Monoamine Oxidase. ACS Chemical Neuroscience, 2019, 10, 3839-3846.	1.7	37
38	One-pot synthesis of high molar activity 6-[18F]fluoro-l-DOPA by Cu-mediated fluorination of a BPin precursor. Organic and Biomolecular Chemistry, 2019, 17, 8701-8705.	1.5	37
39	Identification of [¹⁸ F]TRACK, a Fluorine-18-Labeled Tropomyosin Receptor Kinase (Trk) Inhibitor for PET Imaging. Journal of Medicinal Chemistry, 2018, 61, 1737-1743.	2.9	36
40	Automated synthesis of PET radiotracers by copperâ€mediated ¹⁸ Fâ€fluorination of organoborons: Importance of the order of addition and competing protodeborylation. Journal of Labelled Compounds and Radiopharmaceuticals, 2018, 61, 228-236.	0.5	36
41	Copper(II)-Mediated [¹¹ C]Cyanation of Arylboronic Acids and Arylstannanes. Organic Letters, 2018, 20, 1530-1533.	2.4	35
42	NHC-Copper Mediated Ligand-Directed Radiofluorination of Aryl Halides. Journal of the American Chemical Society, 2020, 142, 7362-7367.	6.6	33
43	Current imaging strategies in rheumatoid arthritis. American Journal of Nuclear Medicine and Molecular Imaging, 2012, 2, 174-220.	1.0	33
44	Synthesis and Evaluation of [¹⁸ F]RAGER: A First Generation Small-Molecule PET Radioligand Targeting the Receptor for Advanced Glycation Endproducts. ACS Chemical Neuroscience, 2016, 7, 391-398.	1.7	32
45	Production of radiometals in liquid targets. EJNMMI Radiopharmacy and Chemistry, 2020, 5, 2.	1.8	32
46	Structural Basis for Achieving GSK-3β Inhibition with High Potency, Selectivity, and Brain Exposure for Positron Emission Tomography Imaging and Drug Discovery. Journal of Medicinal Chemistry, 2019, 62, 9600-9617.	2.9	31
47	Determination of residual Kryptofix 2.2.2 levels in [18F]-labeled radiopharmaceuticals for human use. Applied Radiation and Isotopes, 2007, 65, 1359-1362.	0.7	30
48	Fully automated, high yielding production of <i>N</i> â€succinimidyl 4â€[¹⁸ F]fluorobenzoate ([¹⁸ F]SFB), and its use in microwaveâ€enhanced radiochemical coupling reactions. Journal of Labelled Compounds and Radiopharmaceuticals, 2010, 53, 586-591.	0.5	27
49	A fully-automated one-pot synthesis of [18F]fluoromethylcholine with reduced dimethylaminoethanol contamination via [18F]fluoromethyl tosylate. Applied Radiation and Isotopes, 2013, 78, 26-32.	0.7	27
50	Synthesis and evaluation of [11C]PyrATP-1, a novel radiotracer for PET imaging of glycogen synthase kinase-3β (GSK-3β). Nuclear Medicine and Biology, 2014, 41, 507-512.	0.3	27
51	Iridiumâ€katalysierte Câ€Hâ€Borylierung von Heteroarenen: Eine Balance zwischen sterischer and elektronischer Regiokontrolle. Angewandte Chemie, 2021, 133, 2830-2856.	1.6	27
52	Prevalence of impaired odor identification in Parkinson disease with imaging evidence of nigrostriatal denervation. Journal of Neural Transmission, 2016, 123, 421-424.	1.4	26
53	Synthesis of high-molar-activity [18F]6-fluoro-l-DOPA suitable for human use via Cu-mediated fluorination of a BPin precursor. Nature Protocols, 2020, 15, 1742-1759.	5.5	26
54	Clinical Applications of Small-molecule PET Radiotracers: Current Progress and Future Outlook. Seminars in Nuclear Medicine, 2017, 47, 429-453.	2.5	25

#	Article	IF	CITATIONS
55	Synthesis and Initial In Vivo Evaluation of [11C]AZ683—A Novel PET Radiotracer for Colony Stimulating Factor 1 Receptor (CSF1R). Pharmaceuticals, 2018, 11, 136.	1.7	25
56	An automated method for preparation of [18F]sodium fluoride for injection, USP to address the technetium-99m isotope shortage. Applied Radiation and Isotopes, 2010, 68, 117-119.	0.7	24
57	Intranasal Opioid Administration in Rhesus Monkeys: PET Imaging and Antinociception. Journal of Pharmacology and Experimental Therapeutics, 2016, 359, 366-373.	1.3	23
58	First-in-Human Studies of [¹⁸ F] Fluorohydroxyphenethylguanidines. Circulation: Cardiovascular Imaging, 2018, 11, e007965.	1.3	23
59	Automated production of [11C]acetate and [11C]palmitate using a modified GE Tracerlab FXC-Pro. Applied Radiation and Isotopes, 2011, 69, 691-698.	0.7	22
60	Enhanced radiosyntheses of [11C]raclopride and [11C]DASB using ethanolic loop chemistry. Nuclear Medicine and Biology, 2013, 40, 109-116.	0.3	22
61	(â^')â€{ ¹⁸ F]Flubatine: evaluation in rhesus monkeys and a report of the first fully automated radiosynthesis validated for clinical use. Journal of Labelled Compounds and Radiopharmaceuticals, 2013, 56, 595-599.	0.5	22
62	Green approaches to late-stage fluorination: radiosyntheses of ¹⁸ F-labelled radiopharmaceuticals in ethanol and water. Chemical Communications, 2015, 51, 14805-14808.	2.2	22
63	Regional cerebral cholinergic nerve terminal integrity and cardinal motor features in Parkinson's disease. Brain Communications, 2021, 3, fcab109.	1.5	21
64	Ethanolic carbon-11 chemistry: The introduction of green radiochemistry. Applied Radiation and Isotopes, 2014, 89, 125-129.	0.7	20
65	A Kinome-Wide Selective Radiolabeled TrkB/C Inhibitor for in Vitro and in Vivo Neuroimaging: Synthesis, Preclinical Evaluation, and First-in-Human. Journal of Medicinal Chemistry, 2017, 60, 6897-6910.	2.9	20
66	C–H ¹⁸ F-fluorination of 8-methylquinolines with Ag[¹⁸ F]F. Chemical Communications, 2019, 55, 2976-2979.	2.2	20
67	Evaluation of [¹⁸ F]- <i>N</i> -Methyl lansoprazole as a Tau PET Imaging Agent in First-in-Human Studies. ACS Chemical Neuroscience, 2020, 11, 427-435.	1.7	20
68	A Comprehensive Assessment of ⁶⁸ Ga-PSMA-11 PET in Biochemically Recurrent Prostate Cancer: Results from a Prospective Multicenter Study on 2,005 Patients. Journal of Nuclear Medicine, 2022, 63, 567-572.	2.8	20
69	PSMA PET Validates Higher Rates of Metastatic Disease for European Association of Urology Biochemical Recurrence Risk Groups: An International Multicenter Study. Journal of Nuclear Medicine, 2022, 63, 76-80.	2.8	20
70	First-in-Human Brain Imaging of [¹⁸ F]TRACK, a PET tracer for Tropomyosin Receptor Kinases. ACS Chemical Neuroscience, 2019, 10, 2697-2702.	1.7	19
71	Non-exercise physical activity attenuates motor symptoms in Parkinson disease independent from nigrostriatal degeneration. Parkinsonism and Related Disorders, 2015, 21, 1227-1231.	1.1	18
72	Sequential Ir/Cu-Mediated Method for the <i>Meta</i> -Selective C–H Radiofluorination of (Hetero)Arenes. Journal of the American Chemical Society, 2021, 143, 6915-6921.	6.6	18

#	Article	IF	CITATIONS
73	Tetramethylammonium Fluoride Alcohol Adducts for S _N Ar Fluorination. Organic Letters, 2021, 23, 4493-4498.	2.4	18
74	An updated synthesis of [¹¹ C]carfentanil for positron emission tomography (PET) imaging of the μâ€opioid receptor. Journal of Labelled Compounds and Radiopharmaceuticals, 2017, 60, 375-380.	0.5	17
75	Novel fluorine-18 PET radiotracers based on flumazenil for GABAA imaging in the brain. Nuclear Medicine and Biology, 2013, 40, 901-905.	0.3	15
76	Preclinical Evaluation of ¹¹ C-Sarcosine as a Substrate of Proton-Coupled Amino Acid Transporters and First Human Application in Prostate Cancer. Journal of Nuclear Medicine, 2017, 58, 1216-1223.	2.8	15
77	Deuterium Kinetic Isotope Effect Studies of a Potential in Vivo Metabolic Trapping Agent for Monoamine Oxidase B. ACS Chemical Neuroscience, 2018, 9, 3024-3027.	1.7	15
78	Cerebral topography of vesicular cholinergic transporter changes in neurologically intact adults: A [18F]FEOBV PET study. Aging Brain, 2022, 2, 100039.	0.7	15
79	Synthesis and evaluation of [¹¹ C]PBD150, a radiolabeled glutaminyl cyclase inhibitor for the potential detection of Alzheimer's disease prior to amyloid β aggregation. MedChemComm, 2015, 6, 1065-1068.	3.5	14
80	<i>In Vivo</i> Metabolic Trapping Radiotracers for Imaging Monoamine Oxidase-A and -B Enzymatic Activity. ACS Chemical Neuroscience, 2015, 6, 1965-1971.	1.7	14
81	Radiochemistry, PET Imaging, and the Internet of Chemical Things. ACS Central Science, 2016, 2, 497-505.	5.3	14
82	An updated radiosynthesis of [18F]AV1451 for tau PET imaging. EJNMMI Radiopharmacy and Chemistry, 2017, 2, 7.	1.8	14
83	Synthesis and evaluation of NLRP3-inhibitory sulfonylurea [11C]MCC950 in healthy animals. Bioorganic and Medicinal Chemistry Letters, 2020, 30, 127186.	1.0	14
84	Fluorine-18 patents (2009–2015). Part 2: new radiochemistry. Pharmaceutical Patent Analyst, 2016, 5, 319-349.	0.4	13
85	Automated synthesis of [⁶⁸ Ga]oxine, improved preparation of ⁶⁸ Ga-labeled erythrocytes for blood-pool imaging, and preclinical evaluation in rodents. MedChemComm, 2018, 9, 454-459.	3.5	13
86	Fluorine-18 patents (2009–2015). Part 1: novel radiotracers. Pharmaceutical Patent Analyst, 2016, 5, 17-47.	0.4	12
87	Radiosynthesis of [¹¹ C]LY2795050 for Preclinical and Clinical PET Imaging Using Cu(II)-Mediated Cyanation. ACS Medicinal Chemistry Letters, 2018, 9, 1274-1279.	1.3	12
88	Gallium-68: methodology and novel radiotracers for positron emission tomography (2012–2017). Pharmaceutical Patent Analyst, 2018, 7, 193-227.	0.4	12
89	Development and implementation of ISAR, a new synthesis platform for radiopharmaceutical production. EJNMMI Radiopharmacy and Chemistry, 2019, 4, 24.	1.8	12
90	Use of 55 PET radiotracers under approval of a Radioactive Drug Research Committee (RDRC). EJNMMI Radiopharmacy and Chemistry, 2020, 5, 24.	1.8	12

#	Article	IF	CITATIONS
91	Targeting Metal-Aβ Aggregates with Bifunctional Radioligand [¹¹ C]L2-b and a Fluorine-18 Analogue [¹⁸ F]FL2-b. ACS Medicinal Chemistry Letters, 2015, 6, 112-116.	1.3	11
92	Ring opening of epoxides with [¹⁸ F]FeF species to produce [¹⁸ F]fluorohydrin PET imaging agents. Chemical Communications, 2019, 55, 6361-6364.	2.2	11
93	Strategies for PET imaging of the receptor for advanced glycation endproducts (RAGE). Journal of Pharmaceutical Analysis, 2020, 10, 452-465.	2.4	11
94	Preclinical evaluation of (S)-[18F]GE387, a novel 18-kDa translocator protein (TSPO) PET radioligand with low binding sensitivity to human polymorphism rs6971. European Journal of Nuclear Medicine and Molecular Imaging, 2021, 49, 125-136.	3.3	11
95	Copper-Mediated Radiocyanation of Unprotected Amino Acids and Peptides. Journal of the American Chemical Society, 2022, 144, 7422-7429.	6.6	11
96	Futureproofing [18F]Fludeoxyglucose manufacture at an Academic Medical Center. EJNMMI Radiopharmacy and Chemistry, 2018, 3, 12.	1.8	10
97	Synthesis of [18F]-γ-Fluoro-α,β-unsaturated Esters and Ketones via Vinylogous 18F-Fluorination of α-Diazoacetates with [18F]AgF. Synthesis, 2019, 51, 4401-4407.	1.2	10
98	Potential Applications of Artificial Intelligence and Machine Learning in Radiochemistry and Radiochemical Engineering. PET Clinics, 2021, 16, 525-532.	1.5	10
99	Fully automated radiosynthesis of [11C]PBR28, a radiopharmaceutical for the translocator protein (TSPO) 18kDa, using a GE TRACERIab FXC-Pro. Applied Radiation and Isotopes, 2012, 70, 1779-1783.	0.7	9
100	Radioligands for Tropomyosin Receptor Kinase (Trk) Positron Emission Tomography Imaging. Pharmaceuticals, 2019, 12, 7.	1.7	9
101	Copperâ€Mediated Aminoquinolineâ€Directed Radiofluorination of Aromatic Câ^'H Bonds with K 18 F. Angewandte Chemie, 2019, 131, 3151-3154.	1.6	9
102	Classics in Neuroimaging: Development of Positron Emission Tomography Tracers for Imaging the GABAergic Pathway. ACS Chemical Neuroscience, 2020, 11, 2039-2044.	1.7	9
103	S _N Ar Radiofluorination with In Situ Generated [¹⁸ F]Tetramethylammonium Fluoride. Journal of Organic Chemistry, 2021, 86, 14121-14130.	1.7	9
104	Synthesis of Radiopharmaceuticals via "In-Loop―11C-Carbonylation as Exemplified by the Radiolabeling of Inhibitors of Bruton's Tyrosine Kinase. Frontiers in Nuclear Medicine, 2022, 1, .	0.7	9
105	High-Yielding Automated Convergent Synthesis of No-Carrier-Added [11C-Carbonyl]-Labeled Amino Acids Using the Strecker Reaction. Synlett, 2017, 28, 371-375.	1.0	8
106	Development of Positron Emission Tomography Radiotracers for the GABA Transporter 1. ACS Chemical Neuroscience, 2018, 9, 2767-2773.	1.7	8
107	Breakthroughs in Medicinal Chemistry: New Targets and Mechanisms, New Drugs, New Hopes–6. Molecules, 2020, 25, 119.	1.7	8
108	A spot test for determination of residual TBA levels in ¹⁸ F-radiotracers for human use using Dragendorff reagent. Analytical Methods, 2020, 12, 5004-5009.	1.3	8

#	Article	IF	CITATIONS
109	Radiofluorination of oxazole-carboxamides for preclinical PET neuroimaging of GSK-3. Journal of Fluorine Chemistry, 2021, 245, 109760.	0.9	8
110	Cholinergic brain network deficits associated with vestibular sensory conflict deficits in Parkinson's disease: correlation with postural and gait deficits. Journal of Neural Transmission, 2022, 129, 1001-1009.	1.4	8
111	Training the next generation of radiopharmaceutical scientists. Nuclear Medicine and Biology, 2020, 88-89, 10-13.	0.3	7
112	Classics in Neuroimaging: Imaging the Cholinergic System with Positron Emission Tomography. ACS Chemical Neuroscience, 2021, 12, 1472-1479.	1.7	7
113	Synthesis of 68Ga-radiopharmaceuticals using both generator-derived and cyclotron-produced 68Ga as exemplified by [68Ga]Ga-PSMA-11 for prostate cancer PET imaging. Nature Protocols, 2022, 17, 980-1003.	5.5	7
114	Synthesis and Evaluation of a Fluorine-18 Radioligand for Imaging Huntingtin Aggregates by Positron Emission Tomographic Imaging. Frontiers in Neuroscience, 2021, 15, 766176.	1.4	7
115	A general method for the preparation of perfluoroalkanesulfonyl chlorides. Journal of Fluorine Chemistry, 2005, 126, 1196-1201.	0.9	6
116	Classics in Neuroimaging: Shedding Light on Opioid Receptors with Positron Emission Tomography Imaging. ACS Chemical Neuroscience, 2020, 11, 2906-2914.	1.7	6
117	The Effects of Intramuscular Naloxone Dose on Mu Receptor Displacement of Carfentanil in Rhesus Monkeys. Molecules, 2020, 25, 1360.	1.7	6
118	<i>In Silico</i> Approaches for Addressing Challenges in CNS Radiopharmaceutical Design. ACS Chemical Neuroscience, 2022, 13, 1675-1683.	1.7	6
119	Synthesis of [18F]-Fluorodeoxyglucose ([18F]FDG). , 2012, , 1-13.		5
120	Carbon-11 labeled cathepsin K inhibitors: Syntheses and preliminary in vivo evaluation. Nuclear Medicine and Biology, 2014, 41, 384-389.	0.3	5
121	Targeted nanoparticles for multimodal imaging of the receptor for advanced glycation end-products. Theranostics, 2018, 8, 6352-6354.	4.6	5
122	Breakthroughs in Medicinal Chemistry: New Targets and Mechanisms, New Drugs, New Hopes–7. Molecules, 2020, 25, 2968.	1.7	5
123	Synthesis of 6-[18F]Fluorodopamine (6-[18F]FDA). , 0, , 125-138.		5
124	Synthesis ofL-[methyl-11C]Methionine ([11C]MET). , 0, , 199-212.		5
125	Synthesis of perfluorinated analogs of DOTA and NOTA: bifunctional chelating groups with potential applications in hybrid molecular imaging. Tetrahedron Letters, 2013, 54, 5755-5757.	0.7	4

126 Is logP truly dead?. Nuclear Medicine and Biology, 2017, 54, 41-42.

0.3 4

#	Article	IF	CITATIONS
127	[11C]Carbon Dioxide: Starting Point for Labeling PET Radiopharmaceuticals. , 0, , .		4
128	Fully Automated Radiosynthesis of [¹¹ C]Guanidines for Cardiac PET Imaging. ACS Medicinal Chemistry Letters, 2020, 11, 2325-2330.	1.3	4
129	Radiosynthesis and <i>In Vivo</i> Evaluation of Four Positron Emission Tomography Tracer Candidates for Imaging of Melatonin Receptors. ACS Chemical Neuroscience, 2022, 13, 1382-1394.	1.7	4
130	A novel one-pot palladium-mediated synthesis of N-[(2-hydroxyphenyl)methyl]-N-(4-phenoxy-3-pyridinyl) acetamide, the precursor to [11C]PBR28, a PET biomarker for the peripheral benzodiazepine receptor. Tetrahedron Letters, 2010, 51, 3353-3355.	0.7	3
131	Investigation of Proposed Activity of Clarithromycin at GABA _A Receptors Using [¹¹ C]Flumazenil PET. ACS Medicinal Chemistry Letters, 2016, 7, 746-750.	1.3	3
132	Evaluation of Enzyme Substrate Radiotracers as PET/MRS Hybrid Imaging Agents. ACS Medicinal Chemistry Letters, 2018, 9, 1140-1143.	1.3	3
133	Synthesis and pre-clinical evaluation of a potential radiotracer for PET imaging of the dopamine D3 receptor. MedChemComm, 2018, 9, 1315-1322.	3.5	3
134	Synthesis of 6-(Fluoromethyl)-19-norcholest-5(10)-en-3-ol, a Fluorinated Analogue of NP-59, using the Mild Fluorinating Reagent, TBAF(Pinacol)2. SynOpen, 2019, 03, 55-58.	0.8	3
135	Radionuclide Imaging for Neuroscience: Current Opinion and Future Directions. Molecular Imaging, 2020, 19, 153601212093639.	0.7	3
136	Synthesis of [68Ga]Gallium Dota-(Tyr3)-Octreotide Acetate ([68Ga]-Dotatoc). , 0, , 321-334.		3
137	Radiosynthesis and initial preclinical evaluation of [11C]AZD1283 as a potential P2Y12R PET radiotracer. Nuclear Medicine and Biology, 2022, 114-115, 143-150.	0.3	3
138	Equipment and Instrumentation for Radiopharmaceutical Chemistry. , 2019, , 481-499.		2
139	Improved Synthesis of [¹¹ C]COU and [¹¹ C]PHXY, Evaluation of Neurotoxicity, and Imaging of MAOs in Rodent Heart. ACS Medicinal Chemistry Letters, 2020, 11, 2300-2304.	1.3	2
140	Synthesis of 4-(2′-Methoxyphenyl)-1-[2′-(N-2″Pyridinyl)-p-[18F]Fluorobenzamido]Ethylpiperazine [18F]M , 0, , 87-94.	PPF.	2
141	Synthesis of [11C]-meta-Hydroxyephedrine ([11C]MHED). , 0, , 191-198.		2
142	Synthesis of [18F]FPPRGD2. , 0, , 51-60.		2
143	An updated synthesis of N 1 ′â€{[11 C]methyl)naltrindole for positron emission tomography imaging of the delta opioid receptor. Journal of Labelled Compounds and Radiopharmaceuticals, 2021, 64, 187-193.	0.5	2
144	Besilesomab for imaging inflammation and infection in peripheral bone in adults with suspected osteomyelitis. Reports in Medical Imaging, 2010, , 17.	0.8	1

#	Article	IF	CITATIONS
145	Synthesis of (+)- \hat{l} ±-[11C]Dihydrotetrabenazine ([11C]DTBZ). , 2012, , 213-219.		1
146	Synthesis of [11C]Carfentanil ([11C]CFN). , 2012, , 257-264.		1
147	Guest Editorial. Seminars in Nuclear Medicine, 2017, 47, 427-428.	2.5	1
148	Issues in preclinical radiopharmaceutical research: Significance, relevance and reproducibility. Nuclear Medicine and Biology, 2018, 67, 52-55.	0.3	1
149	Synthesis and Evaluation of ¹¹ C- and ¹⁸ F-Labeled SOAT1 Inhibitors as Macrophage Foam Cell Imaging Agents. ACS Medicinal Chemistry Letters, 2020, 11, 1299-1304.	1.3	1
150	Highlight selection of radiochemistry and radiopharmacy developments by editorial board. EJNMMI Radiopharmacy and Chemistry, 2021, 6, 13.	1.8	1
151	A Picture Is Worth a Thousand Words: The Power of Neuroimaging. ACS Chemical Neuroscience, 2021, 12, 2553-2554.	1.7	1
152	Synthesis of [carbonyl-11C]Way-100635. , 0, , 265-273.		1
153	Synthesis of [18F]Fluoromisonidazole (1-(2-Hydroxy-3-[18F]Fluoropropyl)-2-Nitroimidazole, [18F]FMISO). , 0, , 41-49.		1
154	Clinical Manufacturing of [18F]-16-α-Fluoroestradiol ([18F]FES). , 0, , 69-80.		1
155	Synthesis of [11C]Acetate. , 0, , 297-303.		1
156	No Dopamine Agonist Modulation of Brain [¹⁸ F]FEOBV Binding in Parkinson's Disease. Molecular Pharmaceutics, 2022, 19, 1176-1182.	2.3	1
157	Automated Synthesis of 18F-BCPP-EF {2-tert-Butyl-4-Chloro-5-{6-[2-(2[18F]fluoroethoxy)-Ethoxy]-Pyridin-3-ylmethoxy}-2H-Pyridazin-3-One for Imaging of Mitochondrial Complex 1 in Parkinson's Disease. Frontiers in Chemistry, 2022, 10, 878835.	1.8	1
158	Editorial: Positron Emission Tomography (PET) Imaging of Brain Biochemistry: Beyond High-Affinity Radioligands. Frontiers in Neuroscience, 2022, 16, 907460.	1.4	1
159	A General Method for the Preparation of Perfluoroalkanesulfonyl Chlorides ChemInform, 2005, 36, no.	0.1	Ο
160	Synthesis of [18F]Fluoroethyltyrosine (18F-FET). , 2012, , 103-110.		0
161	Synthesis of [18F]Fluorocholine ([18F]FCH). , 2012, , 61-68.		Ο
162	Synthesis of [18F]Fluoroazomycin Arabinoside ([18F]FAZA). , 2012, , 31-39.		0

#	Article	IF	CITATIONS
163	Synthesis of [13N]Ammonia ([13N]NH3). , 2012, , 313-320.		О
164	Evaluating Cholinergic Receptor Expression in Guinea Pig Primary Auditory and Rostral Belt Cortices After Noise Damage Using [³ H]Scopolamine and [¹⁸ F]Flubatine Autoradiography. Molecular Imaging, 2019, 18, 153601211984892.	0.7	0
165	Linker Selection Tables. , 0, , 589-655.		О
166	Synthesis of 2-(4-N-[11C]Methylaminophenyl)-6-Hydroxybenzothiazole ([11C]6-OH-BTA-1; [11C]PIB). , 0, , 177-189.		0
167	Synthesis of 3-Amino-4-[2-(N-Methyl-N-[11C]Methyl-Amino-Methyl)Phenylsulfanyl]-Benzonitrile ([11C]DASB). , 0, , 285-296.		0
168	Synthesis of [18F]-Substance-P Antagonist-Receptor Quantifier ([18F]SPA-RQ). , 0, , 155-166.		0
169	Synthesis of Sodium [18F]Fluoride (Na[18F]F). , 0, , 15-19.		0
170	Appendix 1: Supplier Information. , 0, , 335-338.		0
171	Synthesis of [11C]Hexadecanoic Acid ([11C]Palmitic Acid). , 0, , 233-243.		0
172	Unnatural amino acids offer new hope for accurate bacterial infection PET imaging in prosthetic joint infection. European Journal of Nuclear Medicine and Molecular Imaging, 0, , .	3.3	0